



## Analysis of Hemodynamic Effect on Different Stent Strut Configuration in Femoral Popliteal Artery during the Physical and Physiological Conditions

Nur Farahalya Razhali<sup>1</sup>, Ishkrizat Taib<sup>1,\*</sup>, Nurul Fitriah Nasir<sup>1</sup>, Ahmad Mubarak Tajul Arifin<sup>1</sup>, Nor Adrian Nor Salim<sup>1</sup>, Shahrul Azmir Osman<sup>1</sup>, Nofrizal Idris Darlis<sup>2</sup>, A. K. Kareem<sup>3</sup>

<sup>1</sup> Faculty of Mechanical and Manufacturing Engineering, Universiti Tun Hussein Onn Malaysia, Parit Raja, 86400 Batu Pahat, Johor, Malaysia

<sup>2</sup> Faculty of Technology, Universiti Tun Hussein Onn Malaysia, Parit Raja, 86400 Batu Pahat, Johor, Malaysia

<sup>3</sup> Department of Biomedical Engineering, Al-Mustaqbal University College, Babylon, Iraq

### ARTICLE INFO

#### Article history:

Received 10 October 2022

Received in revised form 6 December 2022

Accepted 21 December 2022

Available online 30 December 2022

#### Keywords:

Hemodynamics; stent; Peripheral arterial disease; CFD

### ABSTRACT

Peripheral arterial disease (PAD) is a narrowing of the peripheral arteries that might result in blockage if not immediately treated. Normally, an invasive technique called stenting is used at the stenosed arterial region to restore normal blood flow. Thus, it promotes the formation of thrombosis on the stented artery due to the presenting flow recirculation. However, the rate of thrombosis growth was reported to be different for both genders. This is due to an increase in body surface area, body mass index, and weight of the body. Thus, this study aims to investigate the effect of the physiological and physical conditions of men and women with different hemodynamic parameters on the strut configuration in FPA. Five different stent strut configurations were modelled and inserted into the FPA. The computational fluid dynamic (CFD) method was implemented to solve the continuity and N-S equations. The hemodynamic performance of the stent was analyzed based on hemodynamic parameters consisting of time-averaged wall shear stress (TAWSS), time-averaged wall shear stress gradient (TAWSSG), oscillatory shear index (OSI), and relative residence time (RRT). According to the observations, the distal region of the stented FPA had more dominant flow recirculation than the proximal region. The high void area contributed to less growth of the thrombosis.

## 1. Introduction

The Femoral popliteal artery (FPA) is located at the limb of the lower extremity. The primary function of this artery is to carry oxygenated blood from the heart to be supplied to superficial tissues and thigh muscles [1]. The restriction of blood flow in the FPA will cause severe disease in patients known as peripheral artery disease (PAD). PAD is intimately related to chronic inflammatory processes resulting in the formation of lipid plaques or stenosis within arterial walls [2]. The standard treatment of arterial stenosis is by stenting, which effectively props open the artery and thereby

\* Corresponding author.

E-mail address: [iszat@uthm.edu.my](mailto:iszat@uthm.edu.my)

restores blood flow in the diseased vessel [3]. However, in the first month after stent implantation, the restenosis or re-blockage in the artery has already occurred due to atherosclerosis and the growth of thrombosis [4]. Atherosclerosis is the hardening of the arterial wall caused by a build-up of fatty material, while thrombosis is the formation of a blood clot within the lining of an artery, especially in a stented artery. This abnormality of blood movement makes the fatty materials deposit near the stent strut configuration. An arterial injury causes the arterial wall to undergo an episodic process of thrombus formation, arterial inflammation, neointimal hyperplasia, and stent remodeling [5].

A previous study found that a different strut arrangement accelerated atherosclerosis and thrombosis development significantly. The considerable advancement is owing to the fact that each stent has its own strut configuration, which presents variable flow characteristics near the strut [6]. Thus, the significant progress allows the hemodynamic performance of the stent to be predicted. However, Nordstrom *et al* mentioned that, the rate of thrombosis was different between men and women due to increased body surface area, body mass index, and weight for men than women [7]. Furthermore, different vascular regions have presented different flow characteristics that highly depend on the vascular physical condition. Hence, this study was aimed at determining the flow phenomenon near the geometrical pattern of the stent strut configuration to predict the thrombosis growth for different genders and physiological conditions.

The flow process of this research is divided into two sections; simulation and evaluation procedures. In simulation, the simplified geometry of the FPA was developed using computer-aided design (CAD) software to predict the hemodynamic effects of the different stent strut configurations. The computational fluid dynamic (CFD) method was implemented in the modelling to predict the flow behavior by solving the continuity and *Navier-Stokes* equations. The computational fluid dynamic (CFD) method could predict the potential risk of restenosis and WSS distribution in stented arteries [8]. In the second process, this study proposed a detailed analysis and assessment to predict the favorable hemodynamic stent performances among the stents by comparing the hemodynamic variable effects on five different types of commercial stent strut configurations. The hemodynamic variables considered were time-averaged wall shear stress (TAWSS), time-averaged wall shear stress gradient (TAWSSG), oscillating shear index (OSI), and relative residence time (RRT).

## 2. Methodology

### 2.1 Simplified Geometry Model of Stented Femoral Popliteal Artery

The simplified geometry of the FPA artery was developed using the computer aided design (CAD) software SOLIDWORK (Dassault Systèmes SolidWorks Corporation, Waltham, Massachusetts, United States). This model has a length (L) of 109 mm between of proximal and distal end and the diameter (d) of 7.4 mm as shown in Figure 1. The simplified of the FPA was modelled based on the previous finding by Kaha et al [9]. This simplification was made due consideration of the complexity of the strut configuration being inserted at the arterial region. The simplification of the FPA model manage to reduce the computational time which might difficult to reach the convergence if the patient specific geometry is considered.

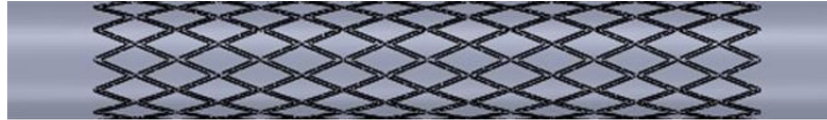


**Fig. 1.** Simplified Femoral Popliteal Artery (FPA)

## 2.2 Meshing of stented femoral popliteal artery model

The stented FPA was meshed using the tetrahedron shapes of mesh and highlighted especially near the strut region as shown in Figure 2. The concentration of the meshing at the strut configuration was through the proximity and curvature methods in order to reach the data accuracy. Patch conforming mesher under tetrahedrons were the most suitable as they captured the curvatures more accurately as compared to other method such as multi zone, hexagonal dominant and sweep. The meshing was generated from 400K to 800K number of nodes in order to improve the quality of the meshing.

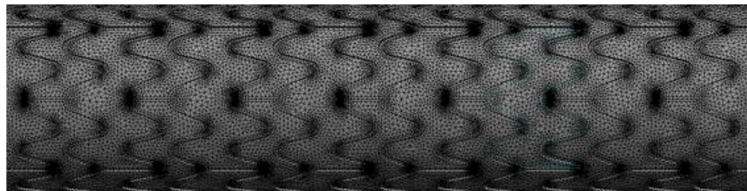


**Fig. 2.** Tetrahedral mesh of the computational domain

## 2.2 Parameter assumptions and boundary condition

In this study, several parameter assumptions were considered in the stented FPA simulation. These assumptions were made to avoid the complexity of unnecessary data being applied on the simulation which might be affected the accuracy of the data. The assumptions parameters were considered as fluid having a constant density of  $1060\text{kg}/\text{m}^3$  and viscosity of  $0.0035\text{ kg}/\text{m}\cdot\text{s}$  [9]. The Reynolds number is the ratio of inertial forces to viscous forces. The value of Reynolds number is 11357, therefore flow is assumed as turbulence only. Since the present study is turbulence, Newtonian blood model is a reasonably good approximation when studying the wall shear stress distribution. In general case, these equations are complex and non-linear, but with suitable assumptions employed for the present study such as incompressibility, a simplified model of equations is obtained. On the solid arterial walls, no-slip boundary condition is imposed. In order to simplify the simulation, the walls of FPA models were assumed rigid as it do not affect the output results significantly.

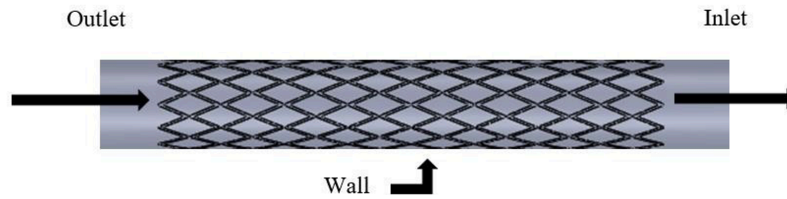


**Fig. 3.** Boundary conditions of stented femoral popliteal artery model

### 2.3 Computational Model and Governing Equation

#### 2.3.1 Time averaged wall shear stress (TAWSS)

The time averaged wall shear stress (TAWSS) was used to quantitatively evaluate the shear stress exerted on the vessel wall around the pulsatile cycle, which can be represented as follows:

$$TAWSS = \frac{1}{T} \int_0^T WSS \, dt \quad (1)$$

where  $t$  is the time and  $T$  is the pulsatile cycle period. A low TAWSS value less than 1 Pa is typically associated with disturbed flow regions, where the flow is slow and changes direction rapidly. A flow with a high TAWSS more than 3 Pa can lead to endothelial trauma, hemolysis, plaque destabilization and ulceration in stenosed vessel [10]. Thus, in this study, analyzed of the TAWSS<sub>low</sub> and TAWSS<sub>high</sub> for the value less than and higher than 1 Pa and 3 Pa respectively. Any value in between 1 Pa and 3 Pa considered as TAWSS<sub>normal</sub>.

#### 2.3.2 Time Averaged Wall Shear Stress Gradient (TAWSSG)

WSSG indicates the formation of new layer of endothelial cells due to different magnitudes of WSS. The desired WSSG value is equal to and less than 5000 Pa/m. Values higher than that could lead to proliferation of endothelial cells and arterial stenosis [11]. Thus, this study has analyzed the WSSG value less than and equal to 5000 N/m<sup>3</sup> in predicting the endothelial cell growth. The computation of WSSG involves WSS derivatives in two directions, which are blood flow direction ( $\alpha$ ) and normal to the direction ( $\beta$ ) as stated in equations (2), (3), (4), (5) and (6). Empirical parameter  $n_A$  denotes the normal to surface area while gradient operator  $\nabla$  is the partial derivative in coordinate direction [12].

$$\alpha = \frac{\tau}{|\tau|} \quad (2)$$

$$\beta = n_A \times \alpha \quad (3)$$

$$\frac{\partial \tau}{\partial \alpha} = \nabla \tau \cdot \alpha \quad (4)$$

$$\frac{\partial \tau}{\partial \beta} = \nabla \tau \cdot \beta \quad (5)$$

$$WSSG = \sqrt{\left(\frac{\partial \tau}{\partial \alpha}\right)^2 + \left(\frac{\partial \tau}{\partial \beta}\right)^2} \quad (6)$$

Since this study is a pulsatile flow, WSSG was computed as TAWSSG as shown in equation (7) [4].

$$TAWSSG = \frac{1}{T} \int_0^T |\overrightarrow{WSSG}| dt \quad (7)$$

### 2.3.3 Oscillatory Shear Index (OSI)

OSI provides an index describing the shear stress that acts in the directions other than that of the temporal mean shear stress vector [13]. The range of OSI for stented artery is from 0 to 0.5. The region with high OSI is predicted to have a high risk of atherosclerosis activity. Since the arterial surfaces with OSI higher than 0.3 are prone to atherosclerosis, the desired value of OSI for better stent performance is from 0.0 to 0.2 [14]. The formulation of the OSI was shown as follows:

$$OSI = \frac{1}{2} \left( 1 - \frac{\left| \int_0^T \overrightarrow{\tau_w} dt \right|}{\int_0^T |\overrightarrow{\tau_w}| dt} \right) \quad (8)$$

### 2.4.4 Relative Residence Time (RRT)

RRT is a scalar-valued quantity that indirectly characterizes the time amount of atherogenic particles to be in contact with arterial wall. Longer time of contact between atherogenic particles and the arterial wall could cause a high prediction on atherosclerosis formation. The atherogenic activity can be seen through RRT higher than  $10 \text{ Pa}^{-1}$  [15,16]. Therefore, the optimum value of RRT for stented hemodynamic model should be less than or equal to  $10 \text{ Pa}^{-1}$ . Thus, RRT was defined as follows [19]:

$$RRT = \frac{1}{(1-2 \times OSI) \times TAWSS} \quad (9)$$

## 3. Result

### 3.1 Grid Independence Test

In this study, five different numbers of nodes were generated as stated in Figure 4. This figure shows the distributions of the velocity at the centerline of the stented FPA for different numbers of nodes within 400k to 800k. From the observation, the suitable numbers of nodes were found at the 532643 nodes. This is due to the smaller truncation error calculated within the range of 400k to 600k. The calculated error was less than 5% the range of the nodes was acceptable.

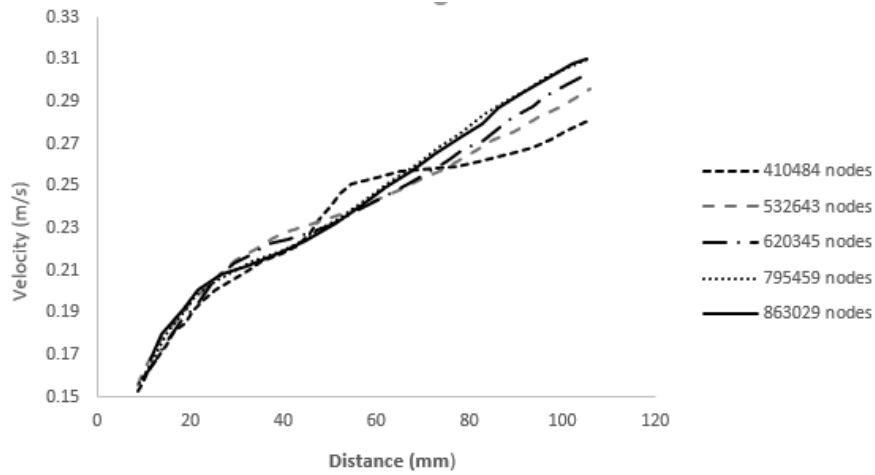


**Fig. 4.** Velocity distributions at the center of femoral popliteal artery for different number of nodes

### 3.2 Validation of Numerical Simulation

In this study, the validation was carried out by validating the streamline of flow velocity in Femoral artery between the present numerical and experimental data by Giurgea *et al.*, [17]. The location of the streamline was taken in the same location. In order to compared the difference. The present numerical study was considered acceptable due to the streamline result of present numerical was almost the same with the streamline result of experimental data with 2% relative error as seen in Figure 5. Thus, the practiced CFD method in numerical simulation setup was valid.

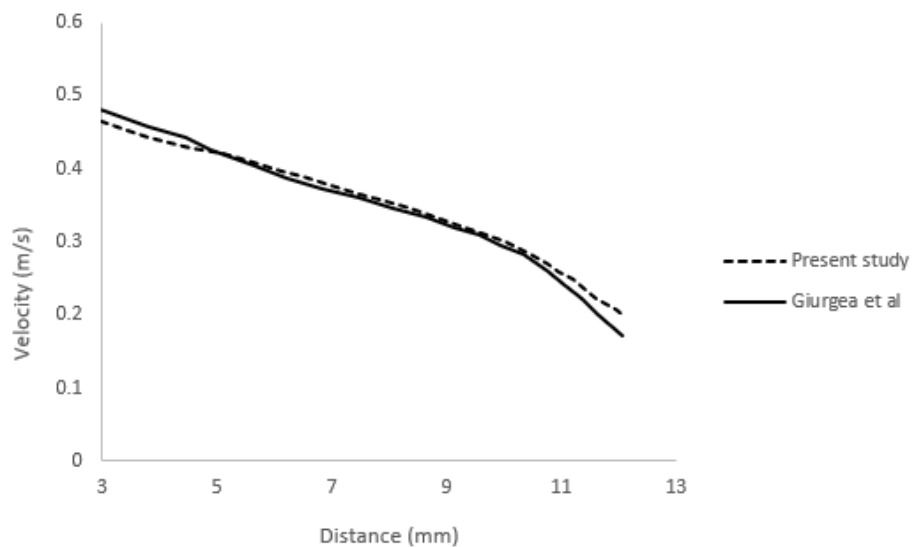


**Fig. 5.** Validation of flow streamline on both present numerical and experimental data

### *3.3 Qualitative Hemodynamic Parameters Distribution on Different Stent Strut Configuration in Femoral Popliteal Artery during Physical and Physiological Condition*

The movement of the blood passing through the corrugated stented FPA caused the chaotic flow characteristic especially near to strut configuration. This phenomenon is caused by WSS which is the important hemodynamic parameter being used to predict the growth of thrombosis. The time-averaged wall shear stress (TAWSS) was introduced to facilitate the quantification and finally predict the hemodynamic stent performance.

The desired WSSG value is equal to and less than 5000 Pa/m. Values higher than that could lead to proliferation of endothelial cells and arterial stenosis. The high WSSG was identified located at the stent strut and the clearest contour appear high WSSG at the stent strut was a man as compared to a woman. In addition, for men case, among all the stents, Type IV stent visualize high WSSG compared to the other stents. Elevated spatial WSSG have been associated with cellular proliferation, and values of WSSG within simulated stents may exceed the threshold required to trigger molecular events associated with neo-intimal hyperplasia [21]. OSI is recognized as a temporal fluctuation of low and high average shear stress in the stented FPA. The highest OSI representing the high risk of the endothelial or wall shear stress affects the formation of plaque [18]. From the observation, the concentration of percentages area of OSI was seen near to strut configuration for both genders. However, the OSI percentage was seen slightly higher in men as compared to women. The OSI value was also shown the highest at the distal regions compared to proximal region due to flow diversion occurred at corrugated stent. In general, the more linkages in the stent strut configuration promotes higher percentages area of OSI.

Relative residence time (RRT) is one of the important hemodynamic parameters which the changes of flow in the artery such as the flow velocity might be affected the growth of the thrombosis after post-operation. In this study, the desired RRT was calculated through the percentages area exposed to the RRT value less than  $10 Pa^{-1}$  [19]. Based on the observation, regions of high RRT were mostly apparent at the location of the strut link.

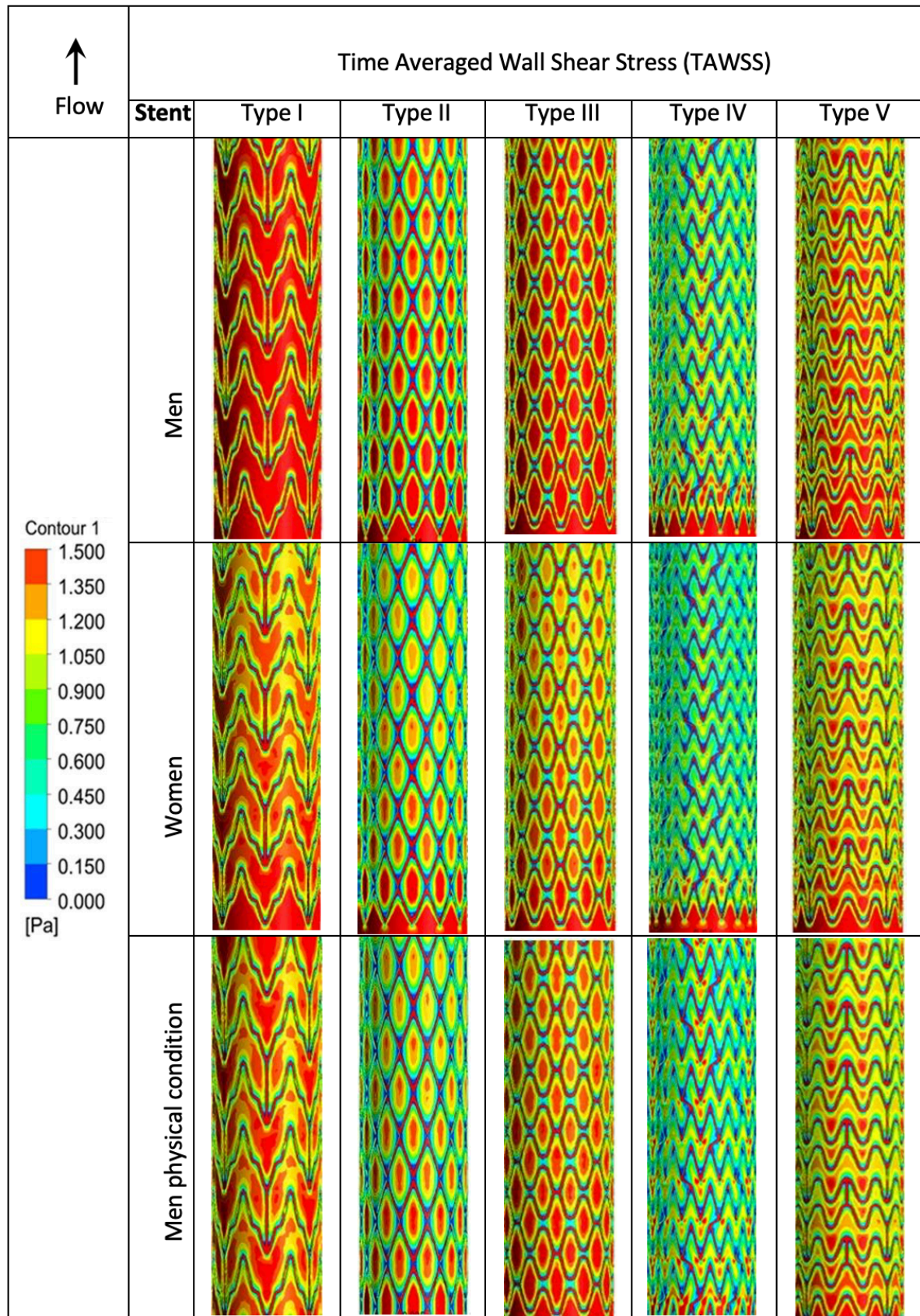


Fig. 6. TAWSS distribution at stent strut configuration for physical and physiological condition



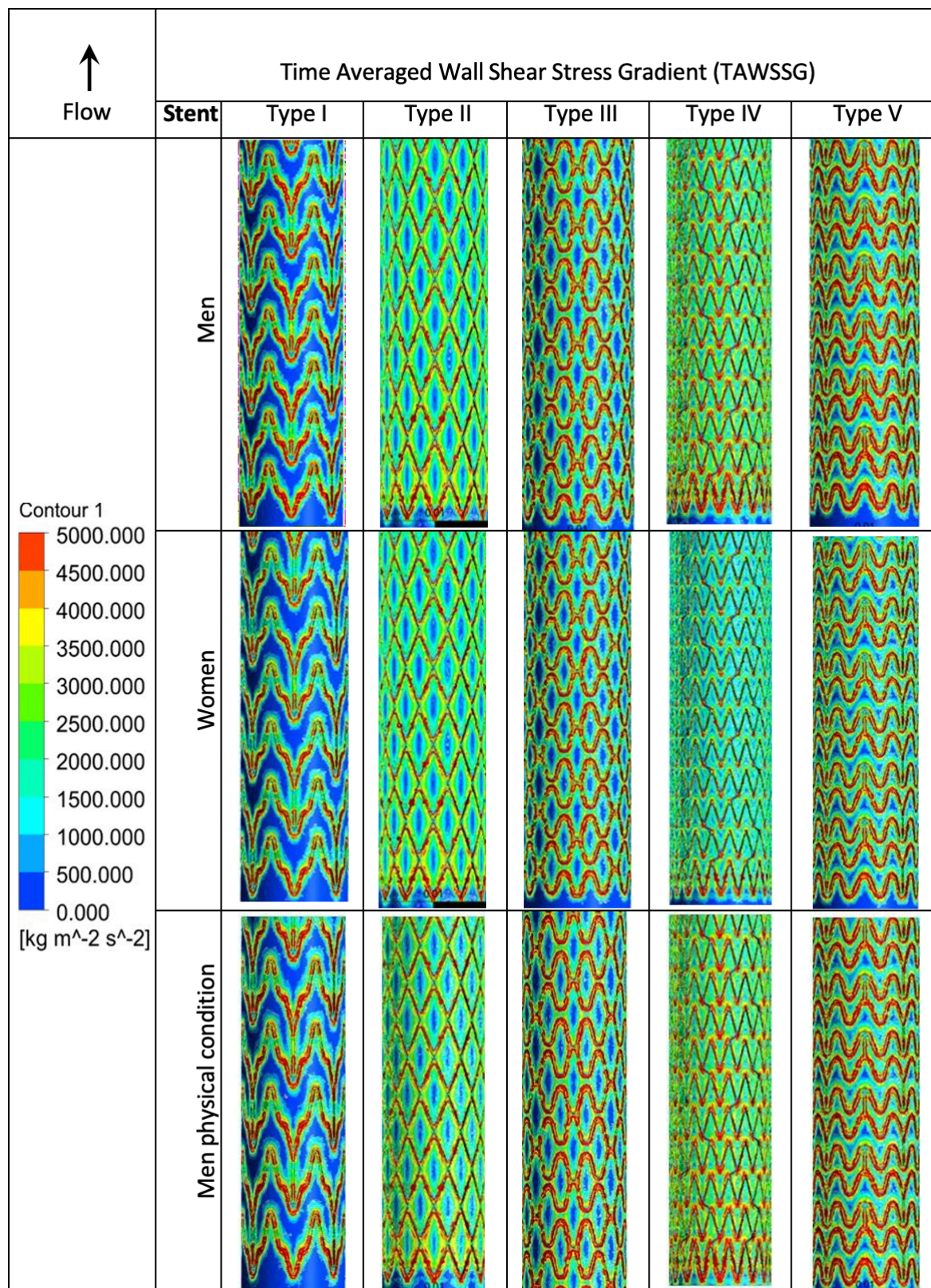


Fig. 7. TAWSSG distribution at stent strut configuration for physical and physiological condition

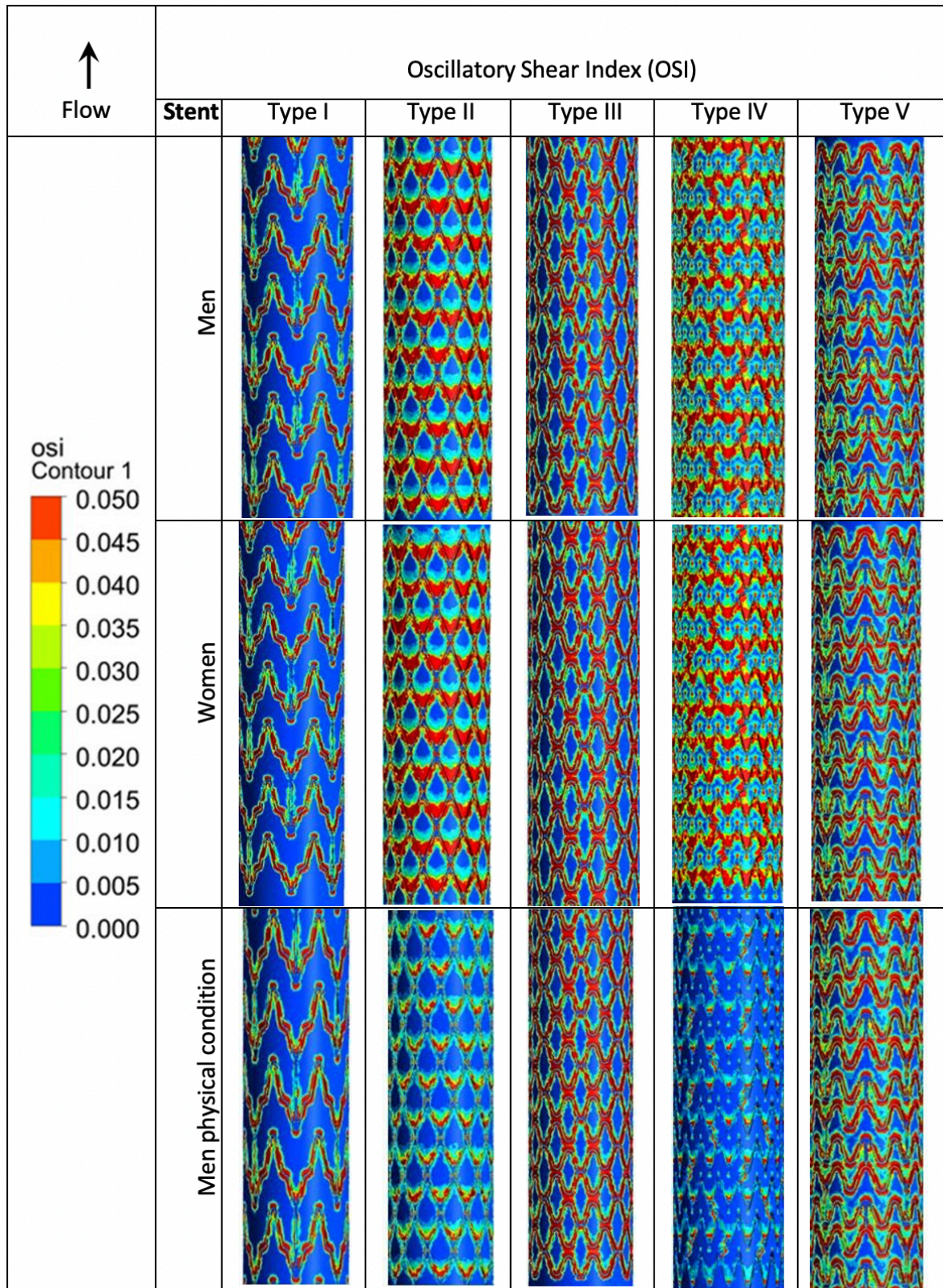


Fig. 8. OSI distribution at stent strut configuration for physical and physiological condition

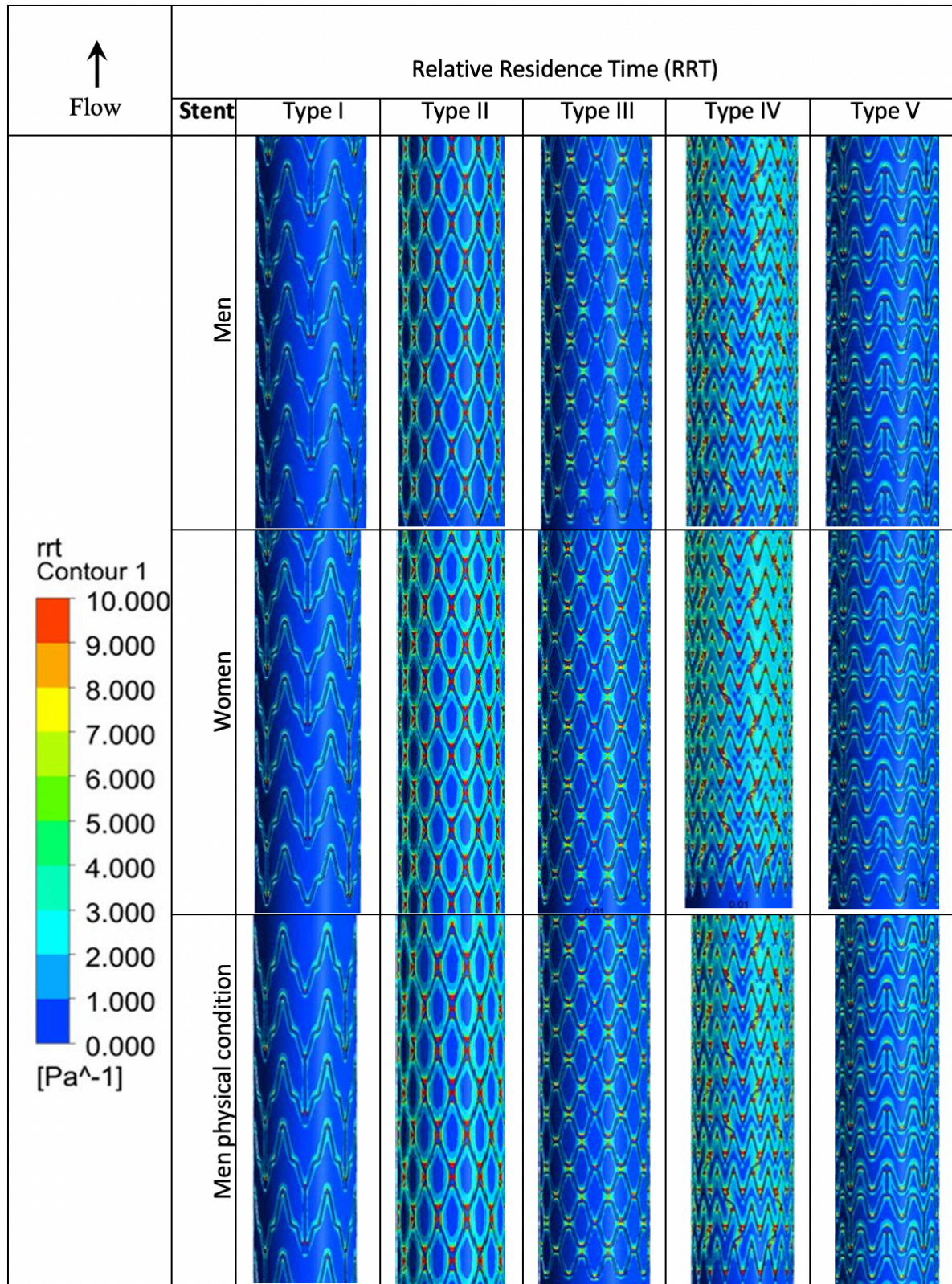


Fig. 9. RRT distribution at stent strut configuration for physical and physiological condition

### 3.4 Quantitative Hemodynamic Parameters Distribution on Different Stent Strut Configuration in Femoral Popliteal Artery during Physical and Physiological Condition

Table 1 shows the percentage of luminal surface area for all hemodynamic parameters. Based on previous studies, the hemodynamic parameters have a specific threshold or range of values to indicate the activity of atherosclerosis and thrombosis that reflect the restenosis development [20-23]. Different critical hemodynamic parameters affect the different flow characteristics due to the variety of stent strut configurations in the femoral popliteal artery and this was aligned with previous studied by Razhali *et al.*, [24]. Thus, the evaluation of restenosis development induced by the flow recirculation due to the misaligned direction of blood flow for different genders and physiological conditions is identified based on the quantitative hemodynamic parameter distribution of different stent strut configuration.

**Table 1**  
 Percentage of luminal surface area for all parameters

Allowable hemodynamic behavior range (%)	Man	Stent	TAWSSlow TAWSS < 1Pa	TAWSSnorm 1 Pa < TAWSS < 3 Pa	TAWSShigh 3 Pa > TAWSS)	TAWSSG TAWSSG ≤ 5000	OSI 0.2 < OSI	RRT 10 < RRT
		Type I	7.62	85.88	5.07	89.93	98.51	98.33
		Type II	20.44	72.07	7.48	89.53	99.81	97.87
		Type III	11.69	83.52	5.28	76.48	99.50	99.61
		Type IV	28.60	62.43	8.95	80.73	99.51	97.46
		Type V	12.9	12.9	5.28	84.09	99.56	99.66
	Women	Stent	TAWSSlow TAWSS < 1Pa	TAWSSnorm 1 Pa < TAWSS < 3 Pa	TAWSShigh 3 Pa > TAWSS	TAWSSG TAWSSG ≤ 5000	OSI 0.2 < OSI	RRT 10 < RRT
		Type I	10.08	86.27	3.63	76.00	99.92	99.69
		Type II	24.5	70.34	5.07	86.01	99.80	97.51
		Type III	14.42	82.10	3.46	84.99	99.49	97.51
		Type IV	34.02	59.70	5.04	83.33	99.48	96.92
		Type V	17.01	79.22	5.28	85.54	99.54	99.34
	Physical Condition	Stent	TAWSSlow TAWSS < 1Pa	TAWSSnorm 1 Pa < TAWSS < 3 Pa	TAWSShigh 3 Pa > TAWSS	TAWSSG TAWSSG ≤ 5000	OSI 0.2 < OSI	RRT 10 < RRT
		Type I	9.17	86.46	4.35	89.93	99.93	98.33
		Type II	23.65	70.33	6.00	85.72	99.81	97.87
		Type III	13.42	83.14	4.02	86.10	99.48	99.61
		Type IV	30.53	61.69	7.76	80.26	99.43	97.46
		Type V	15.56	79.90	4.52	84.08	99.58	99.66

#### 4. Conclusion

In conclusion, the research on investigating the analysis of hemodynamic effects on different stent strut configuration in Femoral Popliteal artery has been successfully carried out. The best stent performance configuration is Type I. Type I stent has high void area contributed to less growth of the thrombosis as compared to the other stent. Thus, this study achieved the aims to investigate the effect of the physiological and physical conditions of men and women with different hemodynamic parameters on the strut configuration in femoral popliteal artery.

#### Acknowledgement

This research was supported by Universiti Tun Hussein Onn Malaysia (UTHM) through FRGS/1/2020/TK0/UTHM/03/38

#### Reference

- [1] Kastrati, Adnan, Julinda Mehilli, Josef Dirschinger, Jürgen Pache, Kurt Ulm, Helmut Schühlen, Melchior Seyfarth et al. "Restenosis after coronary placement of various stent types." *The American journal of cardiology* 87, no. 1 (2001): 34-39. [https://doi.org/10.1016/S0002-9149\(00\)01268-6](https://doi.org/10.1016/S0002-9149(00)01268-6)
- [2] Bentzon, Jacob Fog, Fumiyuki Otsuka, Renu Virmani, and Erling Falk. "Mechanisms of plaque formation and rupture." *Circulation research* 114, no. 12 (2014): 1852-1866. <https://doi.org/10.1161/CIRCRESAHA.114.302721>
- [3] Chen, Xing, Babak Assadsangabi, York Hsiang, and Kenichi Takahata. "Enabling angioplasty-ready "Smart" Stents to detect in-stent restenosis and occlusion." *Advanced Science* 5, no. 5 (2018): 1700560. <https://doi.org/10.1002/advs.201700560>
- [4] Murphy, Jonathan, and Fergal Boyle. "Predicting neointimal hyperplasia in stented arteries using time-dependant computational fluid dynamics: a review." *Computers in biology and medicine* 40, no. 4 (2010): 408-418. <https://doi.org/10.1016/j.combiomed.2010.02.005> Cohen, Barbara J., and Ann DePetris. *Medical terminology: An illustrated guide*. Lippincott Williams & Wilkins, 2013.
- [5] Cohen, Barbara J., and Ann DePetris. *Medical terminology: An illustrated guide*. Lippincott Williams & Wilkins, 2013.
- [6] Paraskevas, Kosmas I., and Frank J. Veith. "Techniques and innovations to improve carotid artery stenting outcomes." *International Journal of Cardiology* 222 (2016): 986-987. <https://doi.org/10.1016/j.ijcard.2016.08.148>
- [7] Nordstrom, Sarah M., and Ethan J. Weiss. "Sex differences in thrombosis." *Expert Review of Hematology* 1, no. 1 (2008): 3-8. <https://doi.org/10.1586/17474086.1.1.3>
- [8] Gökgöl, Can, Nicolas Diehm, Lorenz Räber, and Philippe Büchler. "Prediction of restenosis based on hemodynamical markers in revascularized femoro-popliteal arteries during leg flexion." *Biomechanics and modeling in mechanobiology* 18, no. 6 (2019): 1883-1893. <https://doi.org/10.1007/s10237-019-01183-9>
- [9] Kaha, Asrizan, Muhammad Sufyan Amir Paisal, Ahmad Mubarak Tajul Arifin, Norzelawati Asmuin, Reazul Haq Abdul Haq, Surapong Chatpun, Takahisa Yamamoto, and Kahar Osman. "Lumped Parameter Modelling in Femoral Popliteal Artery for Normal and Severe Conditions." *International Journal of Integrated Engineering* 10, no. 5 (2018). <https://doi.org/10.30880/ijie.2018.10.05.029>
- [10] Wang, I-Chieh, Hsin Huang, Wei-Ting Chang, and Chih-Chung Huang. "Wall shear stress mapping for human femoral artery based on ultrafast ultrasound vector Doppler estimations." *Medical Physics* 48, no. 11 (2021): 6755-6764. <https://doi.org/10.1002/mp.15230>
- [11] Murphy, Jonathan, and Fergal Boyle. "Predicting neointimal hyperplasia in stented arteries using time-dependant computational fluid dynamics: a review." *Computers in biology and medicine* 40, no. 4 (2010): 408-418. <https://doi.org/10.1016/j.combiomed.2010.02.005>
- [12] Mut, Fernando, Rainald Löhner, Aichi Chien, Satoshi Tateshima, Fernando Viñuela, Christopher

- Putman, and Juan R. Cebal. "Computational hemodynamics framework for the analysis of cerebral aneurysms." *International journal for numerical methods in biomedical engineering* 27, no. 6 (2011): 822-839. <https://doi.org/10.1002/cnm.1424>
- [13] Ku, David N., Don P. Giddens, Christopher K. Zarins, and Seymour Glagov. "Pulsatile flow and atherosclerosis in the human carotid bifurcation. Positive correlation between plaque location and low oscillating shear stress." *Arteriosclerosis: An Official Journal of the American Heart Association, Inc.* 5, no. 3 (1985): 293-302. <https://doi.org/10.1161/01.ATV.5.3.293>
- [14] Suess, Taylor, Joseph Anderson, Laura Danielson, Katie Pohlson, Tyler Remund, Elizabeth Blears, Stephen Gent, and Patrick Kelly. "Examination of near-wall hemodynamic parameters in the renal bridging stent of various stent graft configurations for repairing visceral branched aortic aneurysms." *Journal of vascular surgery* 64, no. 3 (2016): 788-796. <https://doi.org/10.1016/j.jvs.2015.04.421>
- [15] Martin, David, and Fergal Boyle. "Sequential structural and fluid dynamics analysis of balloon-expandable coronary stents: a multivariable statistical analysis." *Cardiovascular engineering and technology* 6, no. 3 (2015): 314-328. <https://doi.org/10.1007/s13239-015-0219-9>
- [16] Ng, Jaryl, Christos V. Bourantas, Ryo Torii, Hui Ying Ang, Erhan Tenekecioglu, Patrick W. Serruys, and Nicolas Foin. "Local hemodynamic forces after stenting: implications on restenosis and thrombosis." *Arteriosclerosis, thrombosis, and vascular biology* 37, no. 12 (2017): 2231-2242. <https://doi.org/10.1161/ATVBAHA.117.309728>
- [17] Giurgea, Corina, Florin Bode, Octavian Ioan Budiu, Lucian Nascutiu, Daniel Banyai, and Mihai Damian. "Experimental investigations of the steady flow through an idealized model of a femoral artery bypass." In *EPJ Web of Conferences*, vol. 67, p. 02031. EDP Sciences, 2014. <https://doi.org/10.1051/epjconf/20146702031>
- [18] Chen, Zhiyan, Haiyi Yu, Yue Shi, Minjia Zhu, Yueshen Wang, Xi Hu, Youyi Zhang, Yu Chang, Ming Xu, and Wei Gao. "Vascular remodelling relates to an elevated oscillatory shear index and relative residence time in spontaneously hypertensive rats." *Scientific reports* 7, no. 1 (2017): 1-10. <https://doi.org/10.1038/s41598-017-01906-x>
- [19] Taib, Ishkriyat. "Improvement of Haemodynamic Stent Strut Configuration for Patent Ductus Arteriosus Through Computational Modelling." PhD diss., Universiti Teknologi Malaysia, 2016.
- [20] Murphy, Jonathan B., and Fergal J. Boyle. "A numerical methodology to fully elucidate the altered wall shear stress in a stented coronary artery." *Cardiovascular Engineering and Technology* 1, no. 4 (2010): 256-268. <https://doi.org/10.1007/s13239-010-0028-0>
- [21] Schlager, O., A. Giurgea, C. Margeta, D. Seidinger, S. Steiner-Boeker, B. Van Der Loo, and R. Koppensteiner. "Wall shear stress in the superficial femoral artery of healthy adults and its response to postural changes and exercise." *European Journal of Vascular and Endovascular Surgery* 41, no. 6 (2011): 821-827. <https://doi.org/10.1016/j.ejvs.2011.01.006>
- [22] Kleinstreuer, Clement, Sinjae Hyun, J. R. Buchanan, P. W. Longest, Joseph P. Archie Jr, and George A. Truskey. "Hemodynamic parameters and early intimal thickening in branching blood vessels." *Critical Reviews™ in Biomedical Engineering* 29, no. 1 (2001). <https://doi.org/10.1615/CritRevBiomedEng.v29.i1.10>
- [23] Prado, Cibele M., Simone G. Ramos, Jorge Elias Jr, and Marcos A. Rossi. "Turbulent blood flow plays an essential localizing role in the development of atherosclerotic lesions in experimentally induced hypercholesterolaemia in rats." *International journal of experimental pathology* 89, no. 1 (2008): 72-80. <https://doi.org/10.1111/j.1365-2613.2007.00564.x>
- [24] Razhali, Nur Farahalya, and Ishkriyat Taib. "Analysis of Hemodynamic on Different Stent Strut Configurations in Femoral Popliteal Artery." *CFD Letters* 14, no. 3 (2022): 119-128. <https://doi.org/10.37934/cfdl.14.3.119128>